

Late-Holocene hillslope and fluvial sediment dynamics: a field and modeling approach

Bastiaan Notebaert^{1,2}, Gert Verstraeten^{1,3}

¹Department of Earth & Environmental Sciences, Division of Geography, K.U.Leuven, Belgium, ²Research Foundation Flanders – FWO, Belgium, ³Centre for Archaeological Sciences, K.U.Leuven, Belgium
contact: bastiaan.notebaert@ees.kuleuven.be

1. Introduction

The human impact on sediment fluxes is evidenced by numerous integrated field studies, while the impact of the limited Holocene climate variations in temperate zones remains often unclear. Most of these studies, however, remain qualitative. Detailed field-based approaches have recently been made for several areas that now provide quantitative data. These include time-differentiated catchment sediment budgets, catchment-wide analysis of historic sedimentation rates and cumulative density functions of colluvial and alluvial activity. However, the poor temporal resolution of the sedimentary record makes it in most cases impossible to decipher e.g. the impact of short-lasting climatic events. As a result, the differentiation between land use related and climatic influences based on field data is often problematic. Spatial modeling techniques could provide a means for estimating the impact of past (and future) environmental change on hillslope and fluvial sediment dynamics. In this paper we present a field based and modeling study on Holocene sediment dynamics in the Belgian Dijle catchment.

2. Study Area

The Dijle catchment (760 km²) is situated in the Belgian loess belt in the European temperate zone. First settlements occurred in the region around 5000 BCE. Land use peaked a first time during the Roman Period. Land use intensity peaked again from the Middle Ages onwards, with the major parts of the catchments used for cropland around 1300 CE and again from the 18th century onwards. Two large forest areas were however not deforested since at least the early Middle Ages and provide insight in pre-medieval agriculture and pristine soils.

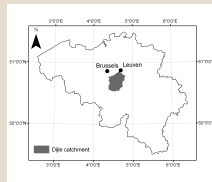


Fig. 2.1: situation of the Dijle catchment (760 km²) within Belgium

3. Field study

3.1 Alluvial deposits

In total 232 hand corings spread over 28 floodplain cross sections were performed to describe Holocene floodplain deposits. The fluvial architecture indicates that vertical floodplain aggradation is the most important Holocene fluvial process in the Dijle catchment. Floodplain deposits typically consist of three important units:

1. an early Holocene peat or organic layer (ca 9000 BCE – 4000 BCE to 1000 CE)
2. an intermediate layer which is less organic (variable – ca 1000 CE)
3. an upper clastic layer (ca 1000 CE – present)

A manual delineation of the floodplain deposits was combined with the coring data to calculate the total mass of floodplain deposits. A correction factor was applied to correct for the presence of organic material.

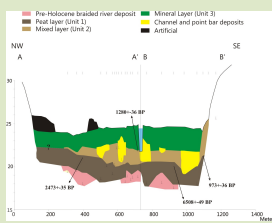


Fig. 3.1: fluvial architecture of the main Dijle floodplain near the outlet of the catchment. Vertical exaggeration: 50 times.

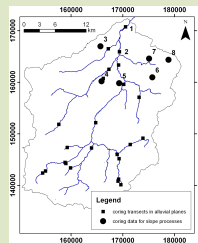


Fig. 3.2: location of floodplain cross sections (1: site of Fig. 3.1) and coring sites on hillslopes (3-9).

3.2 Slope processes

Soil erosion and sediment deposition on slopes was studied using 633 hand augerings for which the thickness of the colluvial layer and the depth of soil horizons were established. The quantity of eroded soil was established by comparison with the ("constant" depth of the same soil horizons under uneroded conditions (soil profile truncation method). Average erosion and deposition quantities were calculated for different morphometrical classes and extrapolated to the entire catchment.

3.3 Dating deposition

Floodplain (12 sites) and colluvial (3 sites) deposition are dated based on 62 radiocarbon and 11 OSL dates, and 29 radiocarbon dates respectively. Dating results are summarized in fig. 3.3. Detailed inspection of site specific deposition shows a close correlation with land use, while no influence of climate could be detected.

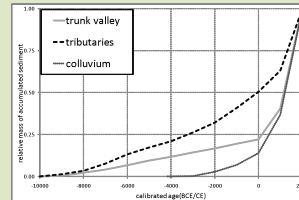


Fig. 3.3: cumulative relative sedimentation curves for the trunk valley floodplain (n=4), tributary floodplains (n=8) and colluvial deposits (n=3).

3.4 Sediment budget

Based on the available data, a time differentiated sediment budget was constructed. Based on the temporal patterns (section 3.3) the budget was differentiated in three periods. Total export out of the catchment was calculated as the difference between total erosion and deposition, and the temporal differences in export are supposed to follow the same pattern as floodplain deposition.

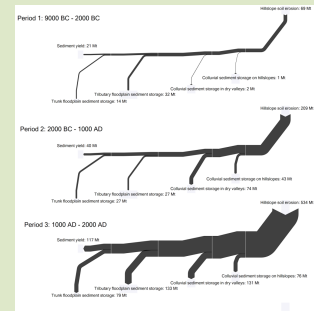


Fig. 3.6: temporal differentiated sediment budget of the Dijle catchment.

5. Conclusions

The combination of the modeling and field approach allows to recognize the important influence of land use on both soil erosion and sediment redistribution, including the changing connectivity of the different parts of the sediment pathway. As a result, the relative importance of sediment sinks also varies over time. The modeling approach allows in addition to quantify the contribution of land use changes, and also to identify and quantify the contribution of climate variations.

More information: Notebaert et al. (2009) Catena, 77: 150-163; Notebaert et al. (2010) Catena, 82: 169-182; Notebaert et al. (2011) Geomorphology, 126: 18-31; Notebaert et al. (in press): Journal of Quaternary Science

4. Modeling study

4.1 Watem/Sedem model

The modeling study was based on the spatially distributed empirical soil erosion and sediment redistribution model Watem/Sedem. Soil erosion calculations are based on the RUSLE formula, while hillslope sediment transport and deposition is modeled using a transport capacity factor. Model input includes topography, land use, climate and soil properties.

4.2 Input Data

An existing calibration of Watem/Sedem using a 100 m pixel resolution and the SRTM DTM was used. Watem/Sedem was applied to different scenarios: pristine (4949–4750 BCE), Neolithic period (3849–3750 BCE), Roman Period (151–250 CE), 1201–1300 CE, 1601–1700 CE, 1701–1800 CE and 1900–1999 CE. A sensitivity analysis was performed in which the different factors are varied individually. Land use is based on the Corine Land Cover (2000 CE), a historical map (1775 CE) and land use reconstruction based on the position of archaeological findings compared to soil types and distance to the stream network. Daily climate data were obtained from the ECBilt-CLIO-VECODE model.

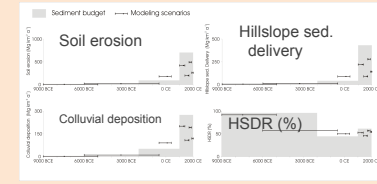


Fig. 4.1: Modeling results compared to the sediment budget.

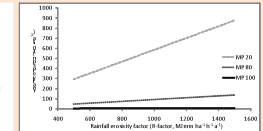


Fig. 4.2: sensitivity analysis: soil erosion in function of rainfall erosivity (X axis) and land use. MP20, MP 80 and MP100 stand for respectively 20, 80 and 100% forest cover.

4.3 Modeling results

Modeling results show a good agreement with the sediment budget (fig. 4.1). Differences are explained by e.g. underestimation of cropland in the land use reconstruction. The sensitivity indicates the important influence of land use on soil erosion and sediment redistribution compared to climate (fig. 4.2, table 4.1). Land use and climatic changes on soil erosion and sediment deposition in the different sinks can be quantified (table 4.1).

An analysis of the temporal variations in HSDR (fig. 4.3) provides further insight in the sediment pathways. Low amounts of erosion can easily be transported under a pristine landscape (high HSDR). Erosion rates locally peak with the introduction of agriculture, but the largely forested landscape is not able to transport these sediment amounts and most of it is deposited as colluvium (low HSDR). With increasing cropland area connectivity between hillslopes and the fluvial system again increases, resulting in a higher HSDR.

Land use	Climate	Erosion rate
Pristine	4950-4851 BCE	100%
Current		106%
de Ferraris map (1775 CE)	4950-4851 BCE	11861%
Current	1700-1799 CE	12099%
Current	4950-4851 BCE	12591%
Current (2000 CE)	Current	6370%

Table 4.1: sensitivity analysis: changes in erosion (as % compared to erosion with a pristine land use and early Holocene climate) for different combinations of land use and climate.

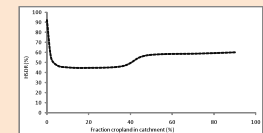


Fig. 4.3: modeling results: HSDR in function of fraction cropland in the catchment